

55th CIRP Conference on Manufacturing Systems

# Additive manufacturing of a passive, sensor-monitored 16MnCr5 steel gear incorporating a wireless signal transmission system

M. Binder<sup>a,b,\*</sup>, V. Stapff<sup>a,c</sup>, A. Heinig<sup>d</sup>, M. Schmitt<sup>a,b</sup>, C. Seidel<sup>a,c</sup>, G. Reinhart<sup>b</sup>

<sup>a</sup>Fraunhofer IGCV (Institute for Casting, Composite and Processing Technology), Am Technologiezentrum 10, 86159 Augsburg, Germany

<sup>b</sup>Technical University of Munich, Institute for Machine Tools and Industrial Management, Boltzmannstr. 15, 85748 Garching, Germany

<sup>c</sup>Munich University of Applied Science, Department of Applied Science and Mechatronics, Lothstr. 34, 80335 Munich, Germany

<sup>d</sup>Fraunhofer IPMS (Institute for Photonic Microsystems), Maria-Reiche-Str. 2, 01109 Dresden, Germany

\* Corresponding author. Tel.: +49 821 90678-192; fax: +49 821 90678-199. E-mail address: [maximilian.binder@igcv.fraunhofer.de](mailto:maximilian.binder@igcv.fraunhofer.de)

## Abstract

The combination of functions in a single component, efficient use of limited space, comprehensive acquisition of process and sensor data and development of passive, wireless monitoring systems are all at the focus of current research. Additive manufacturing is playing an increasingly important role in these developments, because it acts as an enabler for free-form structures, allows access to the interior of the component through its layer-by-layer build-up, and facilitates the processing of a wide variety of materials. Within this work, the aspects mentioned are jointly addressed by the development of a monitored additively manufactured gear (material: 16MnCr5) that communicates wirelessly. This paper shows how an RFID-antenna can be optimized by simulation, incorporated in the design of a metallic gear, then built up in a single manufacturing process and linked to an in-situ inserted sensor board. The approach is validated by fabrication of a sensor-monitored prototype and verified in respect of its functionality and internal structure.

© 2022 The Authors. Published by Elsevier B.V.

This is an open access article under the CC BY-NC-ND license (<https://creativecommons.org/licenses/by-nc-nd/4.0>)

Peer-review under responsibility of the International Programme committee of the 55th CIRP Conference on Manufacturing Systems

**Keywords:** additive manufacturing, sensor integration, RFID-antenna, laser-based powder bed fusion, smart parts, process monitoring, data acquisition

## 1. Introduction

Current fast-growing digital trends, such as condition monitoring and predictive maintenance, increase the pressure on the manufacturing industry to be able to produce components whose condition is monitored by sensors. In this way, maintenance intervals can be minimized and components proactively replaced even before their technical failure [1]. This development involves the need to increase sensor integration for self-monitoring, as well as new requirements for the sensors to be positioned closer to the measured variable, and thus necessitates new solutions [2]. Additive manufacturing (AM) processes, such as the widely used laser-based powder bed fusion of metal powder (PBF-LB/M), offer the possibility of integrating sensors at any point in the component [3] and allow

encapsulated cavity designs corresponding to the sensor geometry [4].

The integration of sensors into components during PBF-LB/M is currently the focus of research [5–7]. In [8] a concept was presented that illustrated how conductive paths can be manufactured using PBF-LB/M and connected to integrated electrical components.

The integration of sensors is becoming increasingly important in all kinds of materials, including metals and fiber-reinforced plastics; equally important is the wireless transmission of data and the passive operation of such systems, for example through use of energy harvesting approaches [9,10].

In previous work, it was demonstrated that the use of insulating powder in cavities containing an integrated sensor can reduce the temperature load from the PBF-LB/M induced

melt pool on the sensor from usually greater than 400 °C to a maximum of 86.2 °C (mean value 48.6 °C) [11]. This approach will be used in this work to protect the electrical component.

16MnCr5 (1.7131) is a low-alloy steel that is widely used in drive trains and gearboxes and can be case-hardened. Using additive manufacturing, the material can be processed reliably and a material density of more than 99.8 % can be achieved [12].

The implementation of a sensor-monitored gear manufactured from 16MnCr5 is intended to address the following technical challenges:

- RFID applications in electromagnetically shielded metal environments,
- Direct acquisition of relevant sensor data (acceleration for vibration analysis) in the machine element to be monitored,
- Additive manufacturing of antenna and loaded component in one process,
- Additive manufacturing of the conductive path between antenna and printed circuit board (PCB)
- Integration of the RFID transponder during the manufacturing process,
- System can be operated passively (battery-free).

By overcoming these challenges, it will be possible in the future to draw conclusions about the lubrication or damage condition of a gear through vibration analysis, but also to record eigenfrequencies of the system or the rotation speed of the gear.

### 1.1. General concept

Of the RFID technologies, UHF (Ultra-high-frequency, 868 MHz) provides a high data rate and long reading range (up to 12 m) compared to LF (Low-frequency, 125 kHz) and HF (High-frequency, 13.56 MHz) with a reading range of few centimeters, making it the most suitable technology for the project. The UHF RFID technology is widespread so that a large selection of components and infrastructure is available for a corresponding system. However, as it is known that electromagnetic waves are strongly shielded by metallic components and, compared to LF technologies, which use inductive coupling, are not able to penetrate metal, this is a major obstacle [13,14]. Therefore, an antenna located on the outside of the gear wheel is to be combined with a well-protected sensor unit positioned inside the gear wheel. In this way, negative shielding effects on the electromagnetic waves can be reduced and the more powerful UHF technology (longer range, faster transmission rate) can be used.

The following components were used to implement the concept (see Figure 1):

- UHF Reader PulsarMX UHF Mid-Range Reader (power transmission: 27 dBm, 500 mW)
- KX122 Tri-Axis Accelerometer (Kionix)
- UHF RFID IC: Rocky100 (860-960 MHz, ISO18000-6 type C compliant, operating temperature between -45 and +85 °C)

The design and additive manufacture of the UHF antenna is described below.

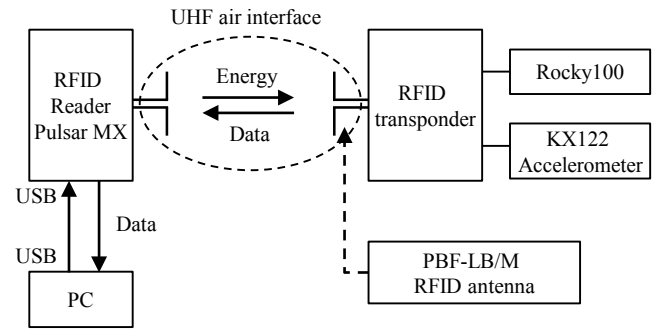


Figure 1: Sketch of the planned RFID communication between the reader and the RFID transponder integrated in the gear wheel.

The tests were carried out on a PBF-LB/M machine of type EOS M290 (EOS GmbH, Germany) and by utilizing prealloyed powder material 16MnCr5 (manufacturer TLS; monomodal particle size distribution with  $d_{10} = 28.42 \mu\text{m}$ ,  $d_{50} = 42.44 \mu\text{m}$  and  $d_{90} = 58.68 \mu\text{m}$ ) was used. The material processing laser energy density was  $86 \text{ J/mm}^3$  at a layer height of  $30 \mu\text{m}$  resulting in a material porosity below 0.5 %, tensile strength of 1050 MPa, yield strength of 1000 MPa and elongation at break of 10.5 % in the as-built state. The hardness (as built) is 330 HV1. [15]

## 2. Concept and antenna layout

The use-case is a straight toothed type C gear with a tip diameter of 118 mm, a bore diameter of 40 mm, 24 teeth and a normal modulus of 4.5. The gear is a typical gear test geometry and is designed for a load of 250 Nm at 3000 rpm. [16]

### 2.1. Antenna and gear concept

Since electromagnetic waves from a UHF RFID source are not known to penetrate metal, a dipole antenna was designed on the outside of the gear, which matches the circular shape of the part. In order to be able to generate the acceleration data inside the gear and to protect the electronic printed circuit board (PCB) from environmental influences such as moisture or oil, a cavity was designed for the sensor integration. The electronics can be installed in the cavity (width: 20 mm, depth: 3,5 mm) during an interruption in the PBF-LB/M process (compare Figure 2). The PCB is configured so that it can be

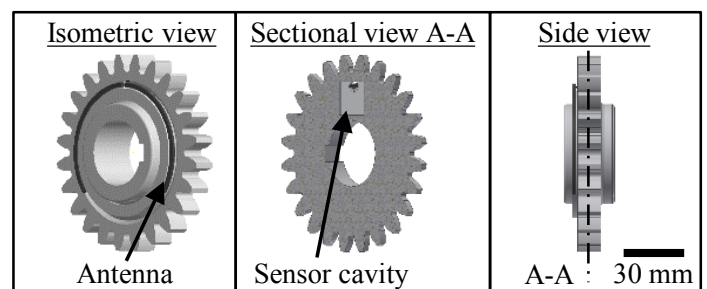


Figure 2: Concept of the external antenna in combination with the internal sensor cavity (gear diameter 118 mm).

electrically connected to the additively built-up antenna during the process interruption (following [8]).

### 2.2. Antenna design

The reader can transmit a legally prescribed maximum energy, a fraction of which is available at the antenna of the transponder. The energy available at the transponder side is essentially determined by the free space attenuation (includes the distance between reader and transponder) and the directional properties of the antenna of the transponder (Gain, see Figure 5). The energy absorbed by the antenna must be fed to the electronic circuit. If the antenna and the input of the electronic circuit are not well coordinated, some of the energy is reflected and not available to the transponder. This adaptation is characterized by the S-parameters of the antenna. To obtain an antenna with good transmission properties, i.e. suitable values for S11 and GAIN, a simulation environment was created in HFSS. HFSS is a 3D electromagnetic simulation software for designing and simulating high-frequency electronic parts provided by ANSYS. The aim is to achieve an S11 smaller than -10 db, which means that 90 % of the energy can be utilized. The dipole antennas used here usually achieve a GAIN of around 2 db, which can, however, be impaired by the metallic environment also involved in the simulation. For this purpose, a design of experiments (DoE) was set up, which allowed for the analysis of the antenna based on four parameters (see Figure 3).

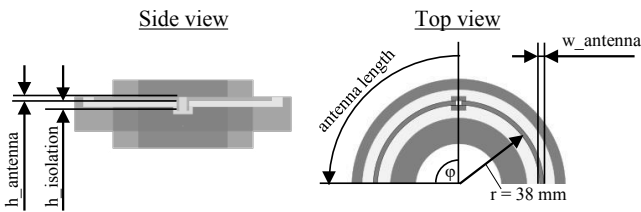


Figure 3: Schematic top view and side view of the gear (teeth not shown). The parameters  $\phi$  (antenna length), antenna width ( $w$ ) antenna height ( $h$ ) and the insulation thickness between the gear and the antenna ( $h_{insulation}$ ) are varied during the simulation.

The parameters were varied systematically and fully factorially in a defined range and the configuration with the best value for the S-parameter was determined (Table 1).

Table 1: Parameters used for a simulative, full-factorial design of experiments. The final configuration corresponds to the configuration with the lowest S-parameter and the highest gain.

	Min.	Max.	Increment	Final config.
$h_{insulation}$ in mm	1	3	0.5	1
$w_{antenna}$ in mm	2	5	0.5	2.6
$h_{antenna}$ in mm	0.3	3	0.3	0.9
$\phi$ in $^\circ$	$60^\circ$	$149^\circ$	$12.7^\circ$	$119.5^\circ$

Figure 4 shows that the final parameter configuration from Table 1 led to a resonance frequency at 868 MHz of the fabricated antenna. The simulation was validated in a measurement chamber where the real read range strongly correlated with the resonance behavior. The slightly different course of the curves is due, among other things, to deviations in the manufacturing accuracy and the surface roughness of the antenna, which were assumed to be idealized in the simulation.

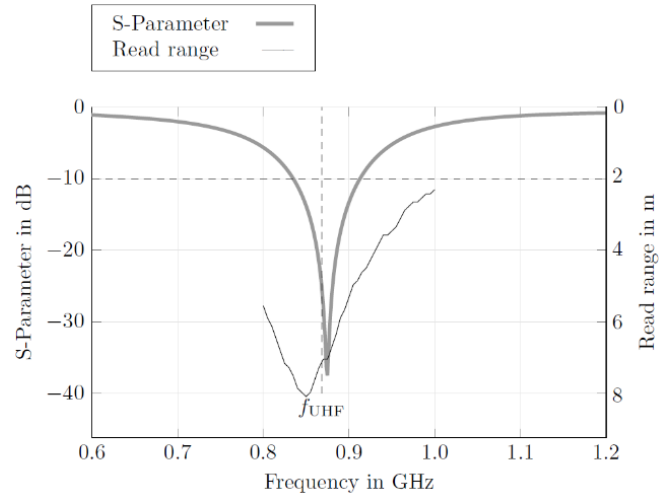


Figure 4: Simulative optimization of the S-Parameter of the antenna and experimental determined read range of the final antenna configuration. Dotted lines: aimed UHF-frequency of 868 MHz and minimum requirement of  $< -10\text{ dB}</math> for the S parameter.$

Figure 5 clearly shows that the radiation pattern of the antenna was not homogeneous and the double lobe is therefore uneven. In particular, this was due to the gear wheel geometry which strongly shields the transmission from the antenna in one direction.

The selected simulation now served as the basis for manufacturing the gear in the next step.

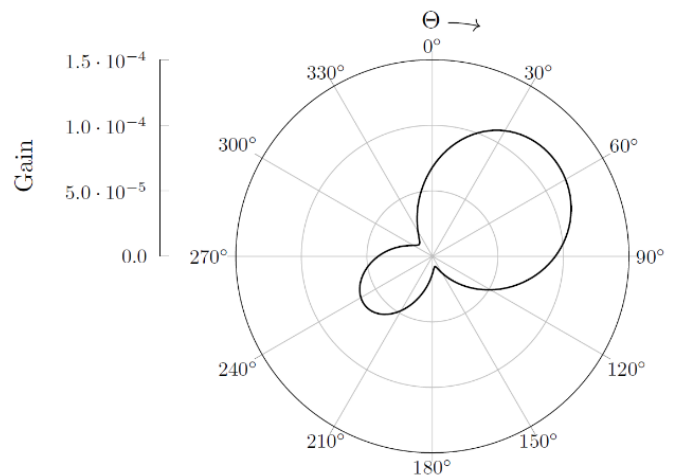


Figure 5: Resulting gain for the simulative designed antenna (final configuration).

### 2.3. Manufacturing via PBF-LB/M

To manufacture the gear, the PBF-LB/M process was started and interrupted at the defined stage (Figure 6, a). A cavity in

the previously built-up part was created by removing powder (b) and the PCB was inserted (c). The additively built-up antenna (material 16MnCr5) was manually soldered to the sensor board in the cavity (c). The cavity was then closed again with powder (d) and the gear manufacturing was completed.

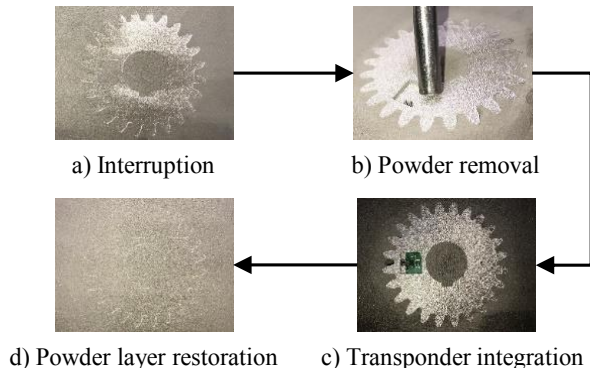


Figure 6: Step-by-step procedure for integrating the PCB when the PBF-LB/M build process was interrupted.

Figure 7 shows the building process in section. The antenna, conductor track and gear wheel can be seen, all made of 16MnCr5. In the interruption layer, the PCB was inserted and electrical connected before the PBF-LB/M process continued. To protect the component, the cavity was sealed with a triangular closure. An opening remained at the tip of the triangle for pouring the insulating compound during the post-process.

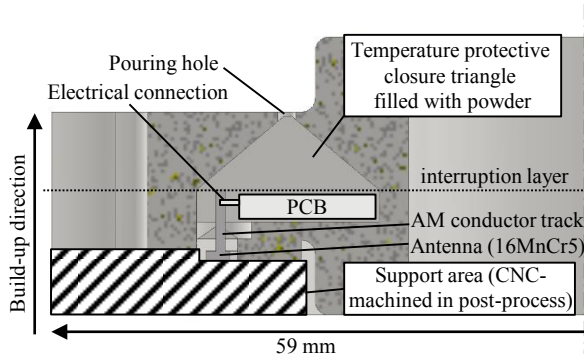


Figure 7: Sectional view through the cavity of the gear wheel during the build-up process.

After the manufacturing process, the gear, which was firmly welded to the build platform, was placed in a depowdering machine (Solukon Maschinenbau GmbH, Germany) for residual powder removal. After this process step the support structures and the antenna surrounding recesses in the gear were free of metal powder. Insulation compound was poured into the gear wheel through a pouring hole, which insulates the antenna, the guide track and the PCB from the surrounding metal (following [8]). After 24 hours, the compound was cured and also fixed the electrical parts in their positions. After the insulator has cured, the entire component was separated from the build platform by wire electrical discharge machining. The antenna was no longer electrically connected to the gear wheel via the build platform, but was isolated together with the other

electrical components in the part (Figure 8). After this step, the finishing was carried out via CNC milling. The entire manufacturing procedure corresponded to the description from [8].

### 3. Validation

As can be seen in Figure 8 a), the gear was successfully manufactured. The powder removal, the contour conforming wire electrical discharge machining, as well as the casting of the insulation compound was implemented as planned. A CT scan (300 kV X-Ray Source) verified that the electrical contact between the antenna and the RFID transponder was successful and that the position of the integrated circuit board was maintained even after casting and curing of the insulation matrix (see Figure 8, b)).

Subsequently, the function of the sensor-monitored gear is ensured by checking the readability of the data. At a distance of 1 cm between the reader and the gear wheel, the data can be read out reliably, even when the gear wheel is rotating (see Figure 9, a)). The gear wheel was rotated with approx. 360°/minute (slow rotation due to a very limited data sampling rate) and the resulting wirelessly transmitted values were read out. As can be seen in Figure 9, b), two sinusoidal curves shifted by  $\pi/2$  relative to each other were generated for the acceleration in the x and y directions under rotation, while the acceleration in the z direction stagnated at 0. These values are plausible and correspond to the expectations of a rotating gear, thereby verifying the correct operation of the system.

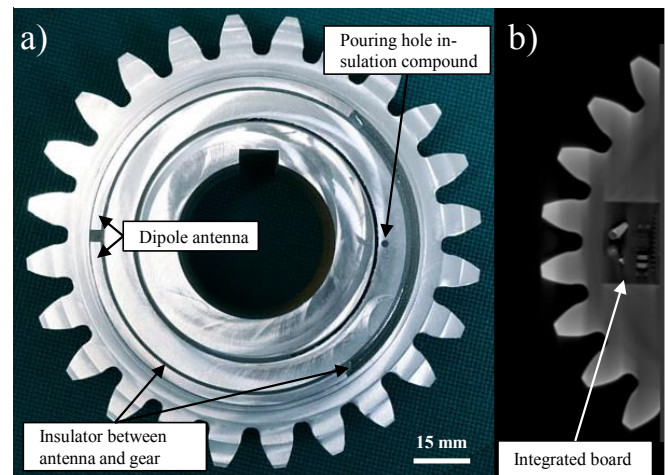


Figure 8: a) manufactured gear (diameter = 118 mm) with marked dipole antenna and present insulation, b) CT scan to verify the right positioning of the integrated PCB in the gear.

### 4. Discussion and outlook

This work has demonstrated how a sensor-monitored, PBF-LB/M fabricated component can be produced by designing an UHF RFID antenna by simulation and extending the standard additive manufacturing process. However, challenges remain for future research:

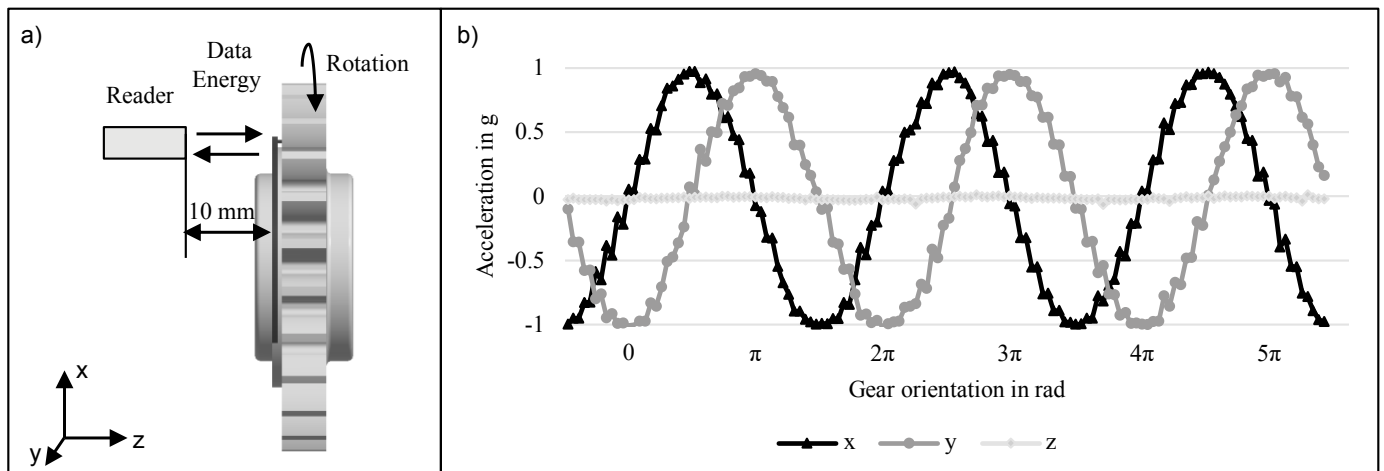


Figure 9: a) Measurement setup of the static read antenna to the rotating gear. b) Wireless transmitted sensor data of the KX122 accelerometer (values of the acceleration in  $g = 9.61 \text{ m/s}^2$  as a function of the gear torsion angle (rad)).

- Post heat treatment: many metal components require thermal treatment after fabrication to achieve the required material properties. For example, for 16MnCr5, stress relief annealing can reduce the gear distortion whereas case-hardening can increase the surface hardness from 350 HV10 up to 750 HV10 (see source [15]). However, up to now a PCB cannot withstand the thermal loads of over 600 °C that occur. Therefore, the focus should either be on the development and use of high temperature resistant sensor technology, the post heat treatment process chain should be avoided by other surface hardening methods like e.g. surface coating techniques or the use of sensor integration should be limited to applications that require less demanding material properties.
- Data transmission rate: to enable vibration monitoring of the component in the future, it must be possible to record and transmit vibrations at a higher frequency. While the system presented in this work is capable of transmitting data at a frequency of 1-2 Hz, for vibration measurement it is desirable to be able to resolve vibrations at  $> 1000 \text{ Hz}$ , otherwise the relevant and high-frequency vibration changes cannot be resolved. Initial approaches for overcoming this challenge are already available and involve using a transponder with an internal controller [17]. Therefore, 1 kHz vibration data could be recorded on the transponder and sent to an external receiver in a rhythm of 10 s (not continuous) or the evaluation could be performed in a decentralized manner in the transponder.
- Reading distance: the maximum readout range was less than expected at  $\sim 1 \text{ cm}$  instead of the desired range of several meters. This is probably due to the electromagnetic field influencing the metal

environment and the rather low achievable gain of the antenna (cf. Fig. 5). In subsequent work, attention should be paid to achieving a higher gain and transmission range by means of an adapted simulation and CAD design of the gear wheel.

It will be possible to transfer the principle to other application components in the future, allowing the advantage of wireless communication to be used with other machine elements and tools. Interesting potential applications include mechanical engineering tools, medical implants or robot grippers and tongs.

#### Acknowledgements

The authors express their sincere thanks to the Federal State of Bavaria and its Bavarian Ministry of Economic Affairs, Regional Development and Energy StMWi for its funding of the "MULTIMATERIAL-Zentrum Augsburg". Process parameters and the gear wheel process chain were developed during the project "Integrational lightweight design for gears by laser beam melting" (RE 1112/50-1) funded by the German Research Foundation (DFG).

#### References

- [1] S. Feldmann, R. Buechele, V. Preveden, Predictive maintenance – From data collection to value creation, München, 2018.
- [2] AMA Fachverband für Sensorik e.V., Sensor-Trends 2014: Trends in zukunftsorientierten Sensortechnologien, Berlin, 2014.
- [3] M.S. Hossain, J.A. Gonzalez, R.M. Hernandez, M.A.I. Shuvo, J. Mireles, A. Choudhuri, Y. Lin, R.B. Wicker, Fabrication of smart parts using powder bed fusion additive manufacturing technology, Additive Manufacturing 10 (2016) 58–66. <https://doi.org/10.1016/j.addma.2016.01.001>.
- [4] D. Mayer, H.A. Stoffregen, O. Heuss, Pöllmann Jennifer, E. Abele, T. Melz, Additive Manufacturing of

- Active Struts for Piezoelectric Shunt Damping, Netherlands, 2014.
- [5] P. Stoll, E. Gasparin, A. Spierings, K. Wegener, Embedding eddy current sensors into LPBF components for structural health monitoring, *Prog Addit Manuf* 26 (2021) 284. <https://doi.org/10.1007/s40964-021-00204-3>.
- [6] S. Bosse, D. Lehmus, W. Lang, M. Busse (Eds.), *Material-integrated intelligent systems: Technology and applications*, Wiley-VCH Verlag GmbH & Co. KGaA, Weinheim, 2018.
- [7] J.F.I. Paz, J. Wilbig, C. Aumund-Kopp, F. Petzoldt, RFID transponder integration in metal surgical instruments produced by additive manufacturing, *Powder Metallurgy* 57 (2014) 365–372. <https://doi.org/10.1179/1743290114Y.0000000112>.
- [8] M. Binder, C. Dirnhofer, P. Kindermann, M. Horn, M. Schmitt, C. Anstaett, G. Schlick, C. Seidel, Gunther Reinhart, Procedure and Validation of the Implementation of Automated Sensor Integration Kinematics in an LPBF System, Chicago, 2020.
- [9] F.-A. Costache, C. Schirrmann, R. Seifert, K. Bornhorst, B. Pawlik, H.-G. Despang, A. Heinig, Polymer Energy Harvester for Powering Wireless communication Systems, *Procedia Engineering* 120 (2015) 333–336. <https://doi.org/10.1016/j.proeng.2015.08.628>.
- [10] A. Weder, S. Geller, A. Heinig, T. Tyczynski, W. Hufenbach, W.-J. Fischer, Integration of Piezoceramic Sensor Elements and Electronic Components in Glass Fibre Reinforced Polyurethane Composite Structures, *Procedia Engineering* 47 (2012) 354–357. <https://doi.org/10.1016/j.proeng.2012.09.156>.
- [11] M. Binder, C. Anstaett, G. Schlick, C. Seidel, R. Wieland, Gunther Reinhart, In-Situ Measurement of the Temperature Progression in Metal Components Manufactured by Laser-based Powder Bed Fusion: Fraunhofer Direct Digital Manufacturing Conference DDMC 2020, ISBN 978-3-8396-1521-8, Berlin, 2020.
- [12] M. Schmitt, B. Kempter, S. Inayathulla, A. Gottwalt, M. Horn, M. Binder, J. Winkler, G. Schlick, T. Tobie, K. Stahl, G. Reinhart, Influence of Baseplate Heating and Shielding Gas on Distortion, Mechanical and Case hardening Properties of 16MnCr5 fabricated by Laser Powder Bed Fusion, *Procedia CIRP* 93 (2020) 581–586. <https://doi.org/10.1016/j.procir.2020.03.089>.
- [13] M. Binder, F. Schönfeld, C. Anstatt, G. Schlick, C. Seidel, G. Reinhart, Radio-Frequency Identification of Metal-AM Parts, Weinheim, 2019.
- [14] K. Finkenzeller, *RFID-Handbuch: Grundlagen und praktische Anwendungen von Transpondern, kontaktlosen Chipkarten und NFC*, 7th ed., Hanser, München, 2015.
- [15] M. Schmitt, T. Kamps, F. Siglmüller, J. Winkler, G. Schlick, C. Seidel, T. Tobie, K. Stahl, G. Reinhart, Laser-based powder bed fusion of 16MnCr5 and resulting material properties, *Additive Manufacturing* 35 (2020) 101372. <https://doi.org/10.1016/j.addma.2020.101372>.
- [16] M. Schmitt, D. Jansen, A. Bihlmeir, J. Winkler, C. Anstatt, G. Schlick, T. Tobie, K. Stahl, G. Reinhart, Rahmen und Strategien für den Leichtbau von additiv gefertigten Zahnrädern für die Automobilindustrie, in: M. Kynast, M. Eichmann, G. Witt (Eds.), *Rapid.Tech + FabCon 3.D International Hub for Additive Manufacturing: Exhibition + Conference + Networking*, Carl Hanser Verlag GmbH & Co. KG, München, 2019, pp. 89–102.
- [17] A. Heinig, Freely programmable UHF sensor transponder circuit: 14.RFID Symposium, Silicon Saxony e.V., Dresden, 2020.